IEEE Access
Multidisciplinary : Rapid Review : Open Access Journal

Received March 13, 2020, accepted March 30, 2020, date of publication April 9, 2020, date of current version April 30, 2020.

Digital Object Identifier 10.1109/ACCESS.2020.2986786

Synchronization of Hyperchaos With Time Delay Using Impulse Control

KUN TIAN[1], HAI-PENG REN[1], (Member, IEEE), AND CHAO BAI[2]
[1]Shaanxi Key Laboratory of Complex System Control and Intelligent Information Processing, Xi'an University of Technology, Xi'an 710048, China
[2]School of Mechatronic Engineering, Xi'an Technological University, Xi'an 710048, China

Corresponding author: Hai-Peng Ren (renhaipeng@xaut.edu.cn)

This work was supported in part by the Shaanxi Provincial Special Support Program for Science and Technology Innovation Leader.

ABSTRACT Secure communication using hyperchaos has a better potential performance, but hyperchaotic impulse circuits synchronization is a challenging task. In this paper, an impulsive control method is proposed for the synchronization of two hyperchaotic Chen circuits with linear or nonlinear delays. Based on the Lyapunov theorem and some analysis techniques, the sufficient conditions for the synchronization of chaotic system with time delay are obtained. The upper bound of the impulse interval is derived to assure the synchronization error system to be asymptotically stable. Simulation and circuit experiment validated the proposed method for correctness and feasibility.

INDEX TERMS Hyperchaotic circuits synchronization, impulse control, linear or nonlinear delays, asymptotically stable theorem.

I. INTRODUCTION

Since Pecora and Carroll presented a pioneering work of chaos synchronization [1], chaos synchronization plays an important role in chaos control. In recent years, chaos synchronization methods have been developed rapidly, such as unidirectionally coupling method [2], OGY (Ott, Grebogi and Yorke) method [3], active control method [4], [5], backstepping control method [6], nonlinear feedback control [7], H_∞ method [8], adaptive feedback control [9], [10], adaptive sliding mode control [11] and impulse control method [12]. It has been studied theoretical and experimental for various kinds of chaotic systems, such as fractional-order systems [13], [14], switched systems [15] and network oscillators [16]. The application of chaos synchronization has been applied in engineering field, e.g., secure communication [17], [18], motor synchronization and vibration compactor [19].

Time delay is a common phenomenon in practical commonplace, such as, communication [22], biology [23] and other fields. In nonlinear dynamics, time delay could generate an infinite dimensional hyperchaos [24], with infinite dimensional structure, promising more application benefits. Time delay could be different forms, including linear time delay or nonlinear time delay, constant or time varying time delay, simple or mixed time delay [20], [21]. Chen system with linear or nonlinear time delay is an example demonstrating multiple kinds of attractors, including the single scroll attractor [25], [26], the double scroll attractors [24], [27] and the composite multi-scroll attractors [22], which possesses multiple positive Lyapunov exponents [25], more complex dynamics, and better application potential. Therefore the combination of the impulse control and Chen system can be applied to encryption, secure communication, spacecraft guidance, etc.. However, the synchronization of the hyperchaotic systems is a challenge task.

Lots of research efforts have been dedicated to impulse control systems. For secure communication [28], [29], the impulse control benefits from significantly decreasing the energy cost and increasing information security. In neural networks [30], the impulse controller is widely applied, because some neurons cannot endure continuous control. Some researchers describe the impulse differential equations by considering the process with the "Jump" state at the beginning [12]. Liu *et al.* employs Lyapunov-Razumikhin theorem and provides the uniform asymptotic stability for the impulse differential equations [31], but they only consider one-dimensional system with time delay [31], [32]. The proof of the global exponential stability for impulse synchronization of network is also presented in [33], which does not consider time delay. In [34], the theoretical results on asymptotic

The associate editor coordinating the review of this manuscript and approving it for publication was Jun Hu.

stability of impulsive systems with time-varying delay are derived, which are quite useful to allow the existence of impulsive perturbations in the chaotic system. However, there is few investigation about impulse synchronization considering the systems with linear/nonlinear multiple time delays. To deal with such problem, in this paper, we have derived the sufficient conditions to assure the synchronization error system are asymptotically stable, which provides the base for the corresponding controller design.

The contribution of this paper is to implement the synchronization between two infinite dimensional hyperchaos systems given by impulse delay differential equations by both simulation and circuit experiment. On the one hand, the uniform asymptotic stability is investigated based on the stability theory of Lyapunov for the hyperchaotic system with linear or nonlinear time delays. Furthermore, the result is extended to other systems with multiple types of time delay.

The rest of the paper is organized as follows. Section 2 gives the theoretical analysis of the stability of impulse synchronization error. Section 3 gives the simulation and experimental results of hyperchaotic system synchronization of the single-scroll attractor in Chen system with linear time delay using the proposed method. Conclusions are given in Section 4.

II. IMPULSE SYNCHRONIZATION OF TIME DELAY INDUCED HYPERCHAOTIC ATTRACTOR

A. PRELIMINARY OF IMPULSE DELAY-DIFFERENTIAL EQUATIONS

In general, an impulsive differential equation is given by

$$\begin{cases} \dot{\boldsymbol{x}} = \boldsymbol{f}(t, \boldsymbol{x}), & t \neq t_k \\ \Delta \boldsymbol{x} = \boldsymbol{x}(t_k^+) - \boldsymbol{x}(t_k^-) = \boldsymbol{I_k}(\boldsymbol{x}), & t = t_k, k \in N \\ \boldsymbol{x}(t_0^+) = \varphi \end{cases} \tag{1}$$

where $\boldsymbol{x}(t) \in R^n$ is state vector, φ is the initial states of $\boldsymbol{x}(t)$, $\boldsymbol{f} : R_+ \times S(\rho) \to R^n$, $\boldsymbol{I_k} : S(\rho) \to R^n$, is continuous function vector on $(t_{k-1}, t_k] \times S(\rho)$, the impulse time t_k satisfy $0 < t_0 < t_1 < t_2 < \ldots$ and $\lim_{k\to\infty} t_k = \infty$. The abbreviated notation $x(t_k^+) = \lim_{t\to t_k^+} x(t)$ and $x(t_k^-) = \lim_{t\to t_k^-} x(t)$ are the right-hand and left-hand limits for time approaching to t_k in forward and reverse direction, respectively.

Assuming that, for all k, $\boldsymbol{f}(t, 0) \equiv 0$ and $\boldsymbol{I_k}(0) = 0$, equation (1) has a trivial solution. The following definitions and lemmas are introduced [31]:

$K_1 = \{g \in C(R_+, R_+) \,|\, g(0) = 0, g(s) > 0, \forall s > 0\}$

$K_2 = \{g \in C(R_+, R_+) \,|$ *is a non-decreasing function and* $g(0) = 0, g(s) > 0,$ *for* $s > 0\}$.

$S(\rho) = \{x \in R^n \,|\, \|x\| < \rho\}$, where $\|\cdot\|$ represents R^n space euclidean norm.

Definition 2.1 [31]: Let $V_0 = \{V : R_+ \times R_+^n \to R_+\}$, $V \in V_0$, *for* $(t, x(t)) \in (nT, (n+1)T) \times R_+^n$, *the upper right derivative of the solution of system* (1) *is defined as* $D^+V[t, x(t)] = \lim_{h\to 0^+} \sup \frac{1}{h} \{V[t+h, x(t)+hf(t, x(t))] - V(t, x(t))\}$

Definition 2.2 [31]: Assume that $r \in N$, $D \subset R$ *and* $F \subset R$, $PC(D, F)$ *denotes a piecewise continuous function from* D *to* F, *namely, if* $\phi \in PC(D, F)$, *when* $t \in D, t \neq t_k$, ϕ *is a continuous function, except* $t = t_k$, ϕ *is a discontinuous function, but left side continuous. Denote* $PC^r(D, F)$ *as* r*-order piecewise global differentiable function from* D *to* F, *namely if* $\phi \in PC^r(D, F)$, *then* $\phi : D \to F$, $\frac{d^r\phi}{dt^r} \in PC(D, F)$.

Lemma 2.1 [31]: Assume existing $a, b, c \in K_1$, $g \in K_2$, $p \in PC(R_+, R_+)$ *and* $V : [-r, \infty) \times S(\rho) \to R_+$, *where* V *is continuous on* $(-r, t_0] \times S(\rho)$ *and* $(t_{k-1}, t_k] \times S(\rho)$, $k = 1, 2, \ldots$, *for each* $x \in S(\rho)$, $k = 0, 1, 2, \ldots$, $\lim_{(t,y)\to(t_k^-,x)} V(t, y) = V(t_k^-, x)$ *exists; V satisfying Lipschitz condition, is restricted on* $R_+ \times S(\rho)$, *if the following conditions hold:*

(1) $b(|\boldsymbol{x}|) \leq V(t, \boldsymbol{x}) \leq a(|\boldsymbol{x}|)$, $(t, \boldsymbol{x}) \in [-r, \infty) \times S(\rho)$;

(2)$D^+V(t, \varphi(0)) \leq p(t)c(V(t, \varphi(0)))$, *for all* $t \neq t_k$ *in* R_+, *and* $\varphi \in PC([-r, 0], S(\rho))$ *whenever* $V(t, \varphi(0)) \geq g(V(t+s, \varphi(s)))$ *for* $s \in [-r, 0]$, *where* $g : R_+^n \to R_+^n$ *is monotone increasing;*

(3)$V(t_k, \varphi(0) + I_k) \leq g(V(t_k^-, \varphi(0)))$ *for all* $(t_k, \varphi) \in R_+ \times PC([-r, 0], S(\rho_1))$, *for which* $\varphi(0^-) = \varphi(0)$;

(4) $\varepsilon = \sup_{k\in z}\{\tau_k - \tau_{k-1}\} < \infty$, *where* ε *is the impulse interval:*

$$W_1 = \sup_{t>0} \int_t^{t+\varepsilon} p(s)ds < \infty,$$
$$W_2 = \inf_{q>0} \int_{g(q)}^{q} \frac{ds}{c(s)} > W_1,$$

then, the trivial solution of system (1) *is uniformly asymptotically stable.*

B. HYPER-CHAOS SYNCHRONIZATION USING IMPULSE CONTROL

For the drive system:

$$\dot{\boldsymbol{x}}(t) = \boldsymbol{A}\boldsymbol{x}(t) + \boldsymbol{B}\boldsymbol{x}(t-\tau) + \boldsymbol{\psi}(\boldsymbol{x}(t)), \tag{2}$$

where $\boldsymbol{A} \in R^{n\times n}$ represents the state matrix, $\boldsymbol{B}$ represents the delay gain matrix, $\boldsymbol{\psi}(\boldsymbol{x})$ represents the nonlinear function, τ represents the delay time. A response system using impulse control is considered as follows:

$$\begin{cases} \dot{\boldsymbol{x}}'(t) = \boldsymbol{A}\boldsymbol{x}'(t) + \boldsymbol{B}\boldsymbol{x}'(t-\tau) + \boldsymbol{\psi}'(\boldsymbol{x}'(t)) & t \neq t_k \\ \Delta \boldsymbol{x}' = \boldsymbol{x}'(t_k^+) - \boldsymbol{x}'(t_k^-) = \boldsymbol{C}_k(\boldsymbol{x}'(t_k) - \boldsymbol{x}(t_k)) & t = t_k, \end{cases} \tag{3}$$

where $\boldsymbol{x}'(t) \in R^n$ represents the state variables, $\Delta\boldsymbol{x}' \in R^n$ represents growth of states under the impulse control at time t_k, $\boldsymbol{C_k} \in R^{n\times n}$ represents impulse control matrix. The matrices A, B are the same as equation (2). From (2) and (3), the synchronization error system is given by:

$$\begin{cases} \dot{\boldsymbol{e}}(t) = \boldsymbol{A}\boldsymbol{e}(t) + \boldsymbol{B}\boldsymbol{e}(t-\tau) + \boldsymbol{\psi}(\boldsymbol{x}(t), \boldsymbol{x}'(t)) & t \neq t_k \\ \Delta \boldsymbol{e}(t) = \boldsymbol{C_k}\boldsymbol{e}(t_k^-) & t = t_k, \end{cases} \tag{4}$$

where $\boldsymbol{e}(t)$ represents $\boldsymbol{e}(t, t-\tau)$, and it denotes $\boldsymbol{e}(t) = \boldsymbol{x}(t) - \boldsymbol{x}'(t)$, $\boldsymbol{\psi}(\boldsymbol{x}(t), \boldsymbol{x}'(t)) = \boldsymbol{\psi}(\boldsymbol{x}(t)) - \boldsymbol{\psi}'(\boldsymbol{x}'(t))$.

In this paper, we will give the theorem for error system (4), by which we can deduce the impulse interval to keep the asymptotically stability of Eq.(4). The uniform asymptotic stability theorem of error system (4) is given as follows.

Theorem 2.1: Considering the error system (4), if there exists a constant l_1 and symmetric and positive defined matrix $\boldsymbol{P}$, such that:

(1) $\|\boldsymbol{\psi}(\boldsymbol{x}(t))\|^2 \le l_1\|\boldsymbol{x}\|^2$.

(2) $W = \frac{\lambda_{\max}(\boldsymbol{A}^T\boldsymbol{P}+\boldsymbol{P}\boldsymbol{A})+2\lambda_{\max}(\boldsymbol{P}^T\boldsymbol{P})}{\lambda_{\min}(\boldsymbol{P})} + \frac{l_1}{\lambda_{\min}(\boldsymbol{P})} + \frac{\|\boldsymbol{B}\|^2\lambda_{\max}(\boldsymbol{P})\lambda_{\min}(\boldsymbol{P})}{\lambda_{\max}((\boldsymbol{I}+\boldsymbol{C_k})^T\boldsymbol{P}(\boldsymbol{I}+\boldsymbol{C_k}))} > 0$,

$0 < \varepsilon < -\frac{\ln(\lambda_{\max}((\boldsymbol{I}+\boldsymbol{C_k})^T\boldsymbol{P}(\boldsymbol{I}+\boldsymbol{C_k}))/\lambda_{\min}(\boldsymbol{P}))}{W}$, where $\lambda_{\max}(\cdot)$ is the maximum eigenvalue of the matrix, $\lambda_{\min}(\cdot)$ is the minimum eigenvalue of the matrix, and ε is the impulse interval.

Then, error system (4) is uniform asymptotically stable.

Proof of Theorem 1:

Select Lyapunov function candidate as:

$$V(x) = \boldsymbol{e}^T\boldsymbol{P}\boldsymbol{e} \tag{5}$$

For $t = t_k$ (6), as shown at the bottom of this page.

here $g(\boldsymbol{V}) = \frac{\lambda_{\max}((\boldsymbol{I}+\boldsymbol{C_k})^T\boldsymbol{P}(\boldsymbol{I}+\boldsymbol{C_k}))}{\lambda_{\min}(\boldsymbol{P})}\boldsymbol{V}$.

If $V(t,\boldsymbol{e}(t)) \ge g(V(t+s,\boldsymbol{e}(t+s)))$, for $-\tau \le s \le 0$, then $V(t,\boldsymbol{e}(t)) \ge \left(\lambda_{\max}\left((\boldsymbol{I}+\boldsymbol{C_k})^T\boldsymbol{P}(\boldsymbol{I}+\boldsymbol{C_k})\right)/\right.$ $\left.\lambda_{\min}(\boldsymbol{P})\right)\cdot V(t+s,\boldsymbol{e}(t+s))$.

Therefore, (7) as shown at the bottom of this page. For $t \ne t_k$ (8), as shown at the bottom of this page.

where

$$p(t) = \frac{\lambda_{\max}\left(\boldsymbol{A}^T\boldsymbol{P}+\boldsymbol{P}\boldsymbol{A}\right)+2\lambda_{\max}\left(\boldsymbol{P}^T\boldsymbol{P}\right)+l_1}{\lambda_{\min}(\boldsymbol{P})} + \frac{\|\boldsymbol{B}\|^2\lambda_{\max}(\boldsymbol{P})\lambda_{\min}(\boldsymbol{P})}{\lambda_{\max}\left((\boldsymbol{I}+\boldsymbol{C_k})^T\boldsymbol{P}(\boldsymbol{I}+\boldsymbol{C_k})\right)},$$

assume $c(s) = s, p(t) = W$

According to condition (4) of Lemma 1, we have:

$$\begin{aligned} W_2 - W_1 &= \inf_{q>0}\int_{g(q)}^{q}\frac{ds}{c(s)} - \sup_{t>0}\int_t^{t+\varepsilon}p(s)\,ds \\ &= \ln q - \ln g(q) - W\varepsilon \\ &= -\ln\frac{\lambda_{\max}\left((\boldsymbol{I}+\boldsymbol{C_k})^T\boldsymbol{P}(\boldsymbol{I}+\boldsymbol{C_k})\right)}{\lambda_{\min}(\boldsymbol{P})} - W\varepsilon > 0 \end{aligned} \tag{9}$$

According to condition (2) of Theorem 1, if the following conditions are established:

$$\begin{aligned} W = &\frac{\lambda_{\max}\left(\boldsymbol{A}^T\boldsymbol{P}+\boldsymbol{P}\boldsymbol{A}\right)+2\lambda_{\max}\left(\boldsymbol{P}^T\boldsymbol{P}\right)}{\lambda_{\min}(\boldsymbol{P})} + \frac{l_1}{\lambda_{\min}(\boldsymbol{P})} \\ &+ \frac{\|\boldsymbol{B}\|^2\lambda_{\max}(\boldsymbol{P})\lambda_{\min}(\boldsymbol{P})}{\lambda_{\max}\left((\boldsymbol{I}+\boldsymbol{C_k})^T\boldsymbol{P}(\boldsymbol{I}+\boldsymbol{C_k})\right)} > 0. \end{aligned} \tag{10}$$

$0 < \varepsilon < -\frac{\ln(\lambda_{\max}((\boldsymbol{I}+\boldsymbol{C_k})^T\boldsymbol{P}(\boldsymbol{I}+\boldsymbol{C_k}))/\lambda_{\min}(\boldsymbol{P}))}{W}$.

Then, we conclude that the error system (4) is asymptotically stability.

End of proof.

Corollary 2.1 (Theorem 1 Can Be Extended to the Delay Differential Equations With Multiple Linear Time Delays):

It is clear that conditions of Theorem 1 is independent of τ. We present Theorem 2 about the system with nonlinear time delays.

Considering the system

$$\dot{\boldsymbol{x}}(t) = \boldsymbol{A}\boldsymbol{x}(t) + \boldsymbol{B}\boldsymbol{x}(t-\tau_1) + \boldsymbol{\psi}(\boldsymbol{x}(t), \boldsymbol{x}(t-\tau_2)) \tag{11}$$

which contains linear and nonlinear time delays, then we have

Theorem 2.2 (Considering Error System of the Equation (11), If There Exists Constants l_1, l_2 and Positive Definite

$$\begin{aligned} V(t_k,\boldsymbol{e}(t_k)) &= \boldsymbol{e}^T(t_k)\boldsymbol{P}\boldsymbol{e}(t_k) \\ &= \left[(\boldsymbol{I}+\boldsymbol{C_k})\boldsymbol{e}(t_k^-)\right]^T\boldsymbol{P}\left[(\boldsymbol{I}+\boldsymbol{C_k})\boldsymbol{e}(t_k^-)\right] \\ &= \boldsymbol{e}(t_k^-)^T\left((\boldsymbol{I}+\boldsymbol{C_k})^T\boldsymbol{P}(\boldsymbol{I}+\boldsymbol{C_k})\right)\boldsymbol{e}(t_k^-) \\ &\le \left[\lambda_{\max}\left((\boldsymbol{I}+\boldsymbol{C_k})^T\boldsymbol{P}(\boldsymbol{I}+\boldsymbol{C_k})\right)/\lambda_{\min}(\boldsymbol{P})\right]\cdot\boldsymbol{e}(t_k^-)^T\boldsymbol{P}\boldsymbol{e}(t_k^-) \\ &\le \left[\lambda_{\max}\left((\boldsymbol{I}+\boldsymbol{C_k})^T\boldsymbol{P}(\boldsymbol{I}+\boldsymbol{C_k})\right)/\lambda_{\min}(\boldsymbol{P})\right]\cdot V\left(t_k^-,\boldsymbol{e}(t_k^-)\right) \\ &= g\left(V\left(t_k^-,\boldsymbol{e}(t_k^-)\right)\right) \end{aligned} \tag{6}$$

$$V(t,\boldsymbol{e}(t)) \ge \left(\lambda_{\max}\left((\boldsymbol{I}+\boldsymbol{C_k})^T\boldsymbol{P}(\boldsymbol{I}+\boldsymbol{C_k})\right)\cdot\lambda_{\max}(\boldsymbol{P})/\lambda_{\min}(\boldsymbol{P})\right)\cdot\|\boldsymbol{e}(t+s)\|^2 \tag{7}$$

$$\begin{aligned} D^+V(\boldsymbol{e}) = &\boldsymbol{e}^T\left(\boldsymbol{A}^T\boldsymbol{P}+\boldsymbol{P}\boldsymbol{A}\right)\boldsymbol{e} + 2\boldsymbol{e}^T\boldsymbol{P}\boldsymbol{B}\boldsymbol{e}(t-\tau) + 2\boldsymbol{e}^T\boldsymbol{P}\boldsymbol{\psi}(\boldsymbol{e}(t)) \\ &\le \left[\lambda_{max}\left(\boldsymbol{A}^T\boldsymbol{P}+\boldsymbol{P}\boldsymbol{A}\right)/\lambda_{min}(\boldsymbol{P})\right]\boldsymbol{e}^T\boldsymbol{P}\boldsymbol{e} + 2\|\boldsymbol{P}\boldsymbol{e}\|^2 + \|\boldsymbol{B}\boldsymbol{e}(t-\tau)\|^2 + \|\boldsymbol{\psi}(\boldsymbol{e}(t))\|^2 \\ &\le \left[\lambda_{max}\left(\boldsymbol{A}^T\boldsymbol{P}+\boldsymbol{P}\boldsymbol{A}\right)\Big/\lambda_{min}(\boldsymbol{P})\right]V(t,\boldsymbol{e}(t)) + 2\|\boldsymbol{P}\boldsymbol{e}\|^2 + \|\boldsymbol{B}\|^2\|\boldsymbol{e}(t-\tau)\|^2 + l_1\|\boldsymbol{e}(t)\|^2 \\ &\le \left[\lambda_{max}\left(\boldsymbol{A}^T\boldsymbol{P}+\boldsymbol{P}\boldsymbol{A}\right)\Big/\lambda_{min}(\boldsymbol{P})\right]V(t,\boldsymbol{e}(t)) + 2\left[\lambda_{max}\left(\boldsymbol{P}^T\boldsymbol{P}\right)\Big/\lambda_{min}(\boldsymbol{P})\right]V(t,\boldsymbol{e}(t)) \\ &\quad + \left[l_1V(t,\boldsymbol{e}(t))\big/\lambda_{min}(\boldsymbol{P})\right] + \|\boldsymbol{B}\|^2\|\boldsymbol{e}(t-\tau)\|^2 \\ &\le \left[\left(\lambda_{max}\left(\boldsymbol{A}^T\boldsymbol{P}+\boldsymbol{P}\boldsymbol{A}\right) + 2\lambda_{max}\left(\boldsymbol{P}^T\boldsymbol{P}\right) + l_1\right)/\lambda_{min}(\boldsymbol{P})\right]\cdot V(t,\boldsymbol{e}(t)) + \|\boldsymbol{B}\|^2\|\boldsymbol{e}(t-\tau)\|^2 \\ &\le p(t)\cdot V(t,\boldsymbol{e}(t)) \end{aligned} \tag{8}$$

Matrix $\boldsymbol{P}$, Such That):
(1) $\|\boldsymbol{\psi}(\boldsymbol{x}(t), \boldsymbol{x}(t-\tau_2))\|^2 \leq l_1\|\boldsymbol{x}(t)\|^2 + l_2\|\boldsymbol{x}(t-\tau_2)\|^2$,
(2) $W = \lambda_{\max}(\boldsymbol{A}^T\boldsymbol{P} + \boldsymbol{P}\boldsymbol{A})/\lambda_{\min}(\boldsymbol{P}) + 2\lambda_{\max}(\boldsymbol{P}^T\boldsymbol{P})/\lambda_{\min}(\boldsymbol{P}) + l_1/\lambda_{\min}(\boldsymbol{P}) + (\|\boldsymbol{B}\|^2 + l_2)\lambda_{\max}(\boldsymbol{P})\lambda_{\min}(\boldsymbol{P})/\lambda_{\max}((\boldsymbol{I}+\boldsymbol{C}_k)^T\boldsymbol{P}(\boldsymbol{I}+\boldsymbol{C}_k))$
$0 < \varepsilon < \frac{-\ln(\lambda_{\max}((\boldsymbol{I}+\boldsymbol{C}_k)^T\boldsymbol{P}(\boldsymbol{I}+\boldsymbol{C}_k))/\lambda_{\min}(\boldsymbol{P}))}{W}$, then the error system is uniform asymptotically stable.

Proof of Theorem 2.2:

Lyapunov function candidate is selected as

$$V(x) = \boldsymbol{e}^T\boldsymbol{P}\boldsymbol{e} \tag{12}$$

The time derivation of (12) at $t = t_k$ is the same as Eq. (8).

For $t \neq t_k$,

$$\begin{aligned} D^+V(\boldsymbol{e}) &= \boldsymbol{e}^T(\boldsymbol{A}^T\boldsymbol{P} + \boldsymbol{P}\boldsymbol{A})\boldsymbol{e} + 2\boldsymbol{e}^T\boldsymbol{P}\boldsymbol{B}\boldsymbol{x}(t-\tau_1) \\ &\quad + 2\boldsymbol{e}^T\boldsymbol{P}\boldsymbol{\psi}(\boldsymbol{e}(t), \boldsymbol{e}(t-\tau_2)) \\ &\leq (\lambda_{\max}(\boldsymbol{A}^T\boldsymbol{P} + \boldsymbol{P}\boldsymbol{A})/\lambda_{\min}(\boldsymbol{P}) + 2\lambda_{\max}(\boldsymbol{P}^T\boldsymbol{P}) \\ &\quad + l_1/\lambda_{\min}(\boldsymbol{P}))\cdot V(t, \boldsymbol{e}(t)) + (\|\boldsymbol{B}\|^2 + l_2)\|\boldsymbol{x}(t-\tau_2)\|^2 \\ &\leq p(t)V(t, \boldsymbol{e}(t)) \end{aligned} \tag{13}$$

where

$$\begin{aligned} p(t) &= \lambda_{\max}(\boldsymbol{A}^T\boldsymbol{P} + \boldsymbol{P}\boldsymbol{A})/\lambda_{\min}(\boldsymbol{P}) + 2\lambda_{\max}(\boldsymbol{P}^T\boldsymbol{P})/\lambda_{\min}(\boldsymbol{P}) \\ &\quad + l_1/\lambda_{\min}(\boldsymbol{P}) + (\|\boldsymbol{B}\|^2 + l_2)\lambda_{\max}(\boldsymbol{P})\lambda_{\min}(\boldsymbol{P})/(\lambda_{\max}((\boldsymbol{I} \\ &\quad + \boldsymbol{C}_k)^T\boldsymbol{P}(\boldsymbol{I}+\boldsymbol{C}_k)) > 0 \end{aligned}$$

denote $c(s) = s$, $p(t) = W$

If the following conditions are established

$$\begin{aligned} W &= \lambda_{\max}(\boldsymbol{A}^T\boldsymbol{P} + \boldsymbol{P}\boldsymbol{A})/\lambda_{\min}(\boldsymbol{P}) + 2\lambda_{\max}(\boldsymbol{P}^T\boldsymbol{P})/\lambda_{\min}(\boldsymbol{P}) \\ &\quad + l_1/\lambda_{\min}(\boldsymbol{P}) + (\|\boldsymbol{B}\|^2 + l_2)\lambda_{\max}(\boldsymbol{P})\lambda_{\min}(\boldsymbol{P})/\lambda_{\max}((\boldsymbol{I} \\ &\quad + \boldsymbol{C}_k)^T\boldsymbol{P}(\boldsymbol{I}+\boldsymbol{C}_k)) > 0 \\ 0 &< \varepsilon < \frac{-\ln(\lambda_{\max}((\boldsymbol{I}+\boldsymbol{C}_k)^T\boldsymbol{P}(\boldsymbol{I}+\boldsymbol{C}_k))/\lambda_{\min}(\boldsymbol{P}))}{W} \end{aligned}$$

Then, with a similar process to the proof of Theorem 2.1, we conclude that the error system of equation (11) is asymptotically stability.

End of Proof

III. SIMULATION AND CIRCUIT EXPERIMENT RESULTS

A. HYPER-CHAOTIC SINGLE-SCROLL ATTRACTOR IN CHEN SYSTEM WITH TIME-DELAY

Chen system with linear time delay feedback is given as follows [27]:

$$\begin{cases} \dot{x}(t) = a(y(t) - x(t)); \\ \dot{y}(t) = (c-a)x(t) - x(t)z(t) + cy(t); \\ \dot{z}(t) = x(t)y(t) - bz(t) + k(z(t) - z(t-\tau)) \end{cases} \tag{14}$$

With different parameters, Chen system with time delay demonstrates four kinds of attractors, such as single scroll attractor(in Fig.1(a)), double scroll attractor (in Fig.1(b)), multi-scroll attractor(in Fig.1(c)) and D-scroll attractor(in Fig.1(d)). The parameters configuration are presented as shown in Table 1. The idea of the impulse synchronization for Chen system with time delay will gain better insight into the image encryption and secure communication [22].

TABLE 1. Parameters configuration values.

	a	b	c	k	τ
single-scroll attractor	35	3	18.35978	2.85	0.3
double-scroll attractor	35	3	18.5	2.85	0.3
multi-scroll attractor	35	3	18.5	3.8	0.3
D–scroll attractor	34.9	3	18.5	2.95	0.336

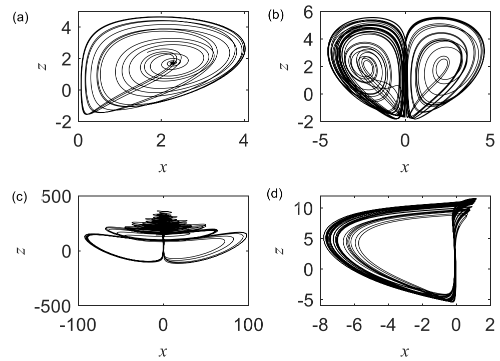

FIGURE 1. The multi-kind of attractors in Chen system with time delay, (a)single-scroll attractor, (b)double-scroll attractor, (c)multi-scroll attractor, (d)D-scroll attractor.

B. SIMULATION RESULTS

1) SYNCHRONIZATION OF CHEN SYSTEMS WITH LINEAR TIME DELAY USING IMPULSE CONTROL

Chen system with linear time delay feedback control can be given as:

$$\dot{\boldsymbol{x}}(t) = \boldsymbol{A}\boldsymbol{x}(t) + \boldsymbol{B}\boldsymbol{x}(t-\tau) + \boldsymbol{\psi}(\boldsymbol{x}(t)), \tag{15}$$

where

$$\boldsymbol{x} = \begin{bmatrix} x \\ y \\ z \end{bmatrix}, \quad \boldsymbol{A} = \begin{bmatrix} -35 & 35 & 0 \\ -17 & 18 & 0 \\ 0 & 0 & -3+K \end{bmatrix},$$
$$\boldsymbol{B} = \begin{bmatrix} 0 & 0 & 0 \\ 0 & 0 & 0 \\ 0 & 0 & -K \end{bmatrix}, \quad \boldsymbol{\psi}(\boldsymbol{x}(t)) = \begin{bmatrix} 0 \\ -x(t)z(t) \\ x(t)y(t) \end{bmatrix},$$
$$K = 3.8, \quad \tau = 0.3.$$

The response system with impulse control is given as follows:

$$\begin{cases} \dot{\boldsymbol{x}}'(t) = \boldsymbol{A}\boldsymbol{x}'(t) + \boldsymbol{B}\boldsymbol{x}'(t-\tau) + \boldsymbol{\psi}\left(\boldsymbol{x}'(t)\right) & t \neq t_k \\ \Delta\boldsymbol{x}' = \boldsymbol{x}'\left(t_k^+\right) - \boldsymbol{x}'\left(t_k^-\right) = \boldsymbol{C}\left(\boldsymbol{x}'(t_k) - \boldsymbol{x}(t_k)\right) & t = t_k, \end{cases} \tag{16}$$

where $\boldsymbol{\psi}'\left(\boldsymbol{x}'(t)\right) = \begin{bmatrix} 0 \\ -x'z' \\ x'y' \end{bmatrix}$, $\boldsymbol{x}' = \begin{bmatrix} x' \\ y' \\ z' \end{bmatrix}$, $\boldsymbol{A}$ and $\boldsymbol{B}$ are the same as that in Eq. (18).

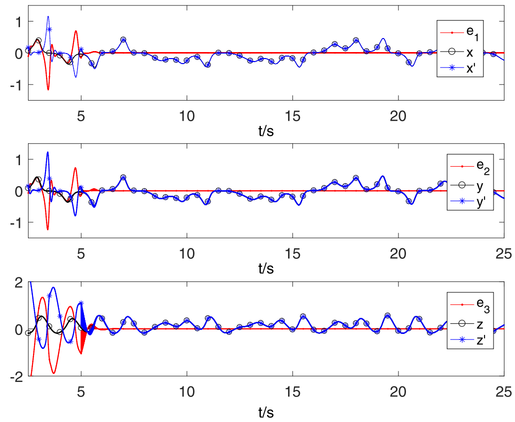

FIGURE 2. Simulation waveform of synchronization of the Chen system with linear time delay using impulse control.

The error system is given by:

$$\begin{cases} \dot{\boldsymbol{e}}(t) = \boldsymbol{A}\boldsymbol{e}\,(t) + \boldsymbol{B}\boldsymbol{e}(t-\tau) + \boldsymbol{\psi}'\left(\boldsymbol{x}, \boldsymbol{x}'\right) & t \neq t_k \\ \Delta \boldsymbol{e} = \boldsymbol{C}\boldsymbol{e}\left(t_k^-\right) & t = t_k, \end{cases} \tag{17}$$

where $\boldsymbol{e}(t) = \boldsymbol{x}(t) - \boldsymbol{x}'(t)$, $\boldsymbol{\psi}\left(\boldsymbol{x}, \boldsymbol{x}'\right) = \boldsymbol{\psi}\,(\boldsymbol{x}) - \boldsymbol{\psi}'\left(\boldsymbol{x}'\right)$, $\boldsymbol{A}$, $\boldsymbol{B}$ are the same as that in Eq. (18).

Impulse control matrix $\boldsymbol{C} = \begin{pmatrix} -0.2 & 0 & 0 \\ 0 & -1.8 & 0 \\ 0 & 0 & -1.8 \end{pmatrix}$, for convenience, let $\boldsymbol{P} = I$. $\|\boldsymbol{\psi}\,(\boldsymbol{x}\,(t))\|^2 \leq l_1 \|\boldsymbol{x}\|^2 = 16\|\boldsymbol{x}\|^2$, thus condition (1) in Theorem 1 is satisfied.

From condition (2) in Theorem 1, we have,

$(1) W = \frac{\lambda_{\max}(\boldsymbol{A}^T\boldsymbol{P}+\boldsymbol{P}\boldsymbol{A})+2\lambda_{\max}(\boldsymbol{P}^T\boldsymbol{P})+l_1}{\lambda_{\min}(\boldsymbol{P})}$ $+\frac{\|\boldsymbol{B}\|^2\lambda_{\max}(\boldsymbol{P})\lambda_{\min}(\boldsymbol{P})}{\lambda_{\max}((\boldsymbol{I}+\boldsymbol{C}_k)^T\boldsymbol{P}(\boldsymbol{I}+\boldsymbol{C}_k))} = \frac{38.9732+2+16}{1} + \frac{14.44}{0.64} = 79.5357$

$(2) 0 < \varepsilon < -\frac{\ln\left(\lambda_{\max}\left((\boldsymbol{I}+\boldsymbol{C}_k)^T\boldsymbol{P}(\boldsymbol{I}+\boldsymbol{C}_k)\right)/\lambda_{\min}(\boldsymbol{P})\right)}{W} = -\frac{\ln(0.64)}{79.5357}$ $= 0.005611.$

In order to meet the conditions in Theorem 2.1, the impulse interval is selected as $\varepsilon = 0.005$. The initial states of the two systems are specified as $(\boldsymbol{x}(0), \boldsymbol{x}'(0)) = ((0.1, 0.1, -0.1), (0.2, 0.2, 5))$. The simulation results are given in Fig. 2, the impulse control is activated from $t = 5s$. The subplot (a) gives the curves of states x of drive system, x' of response system and the state error e_1 in black line with circle, blue line with star and red line with dot, respectively. From Fig. 2, we know that the synchronization is achieved after the impulse controller is active at $t = 5$s.

2) SYNCHRONIZATION OF CHEN SYSTEMS WITH NONLINEAR TIME DELAY USING IMPULSE CONTROL

Chen system with nonlinear time delay feedback control can be given as:

$$\dot{\boldsymbol{x}}(t) = \boldsymbol{A}\boldsymbol{x}(t) + \boldsymbol{B}\boldsymbol{x}(t-\tau_1) + \boldsymbol{\psi}(\boldsymbol{x}(t), \boldsymbol{x}(t-\tau_2)), \tag{18}$$

where

$$\boldsymbol{x} = \begin{bmatrix} x \\ y \\ z \end{bmatrix}, \quad \boldsymbol{A} = \begin{bmatrix} -35 & 35 & 0 \\ -17 & 18 & 0 \\ 0 & 0 & -3+K \end{bmatrix},$$

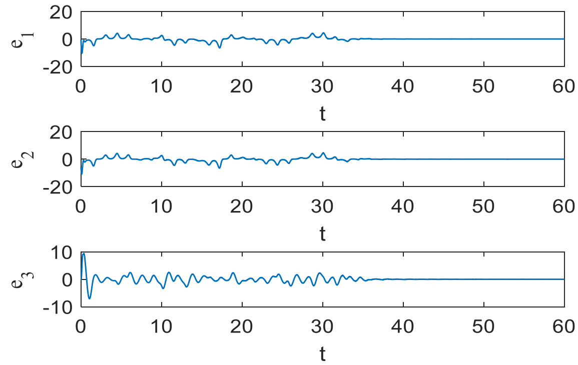

FIGURE 3. Simulation waveform of synchronization of the Chen system with nonlinear time delay using impulse control.

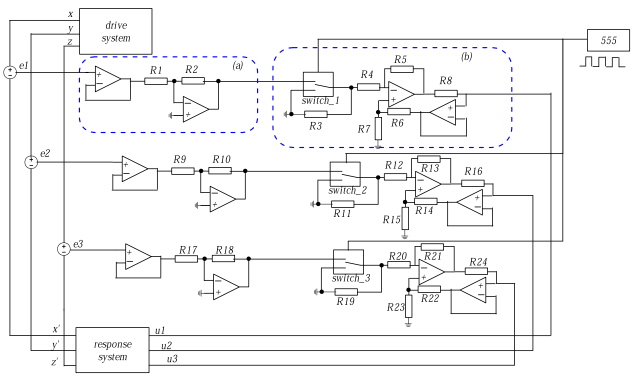

FIGURE 4. Schematic diagram of the impulse control.

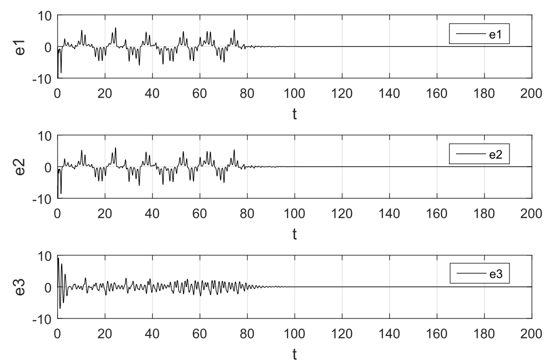

FIGURE 5. Simulation waveform of synchronization of the Chen circuit with time delay using impulse control.

$$\boldsymbol{B} = \begin{bmatrix} 0 & 0 & 0 \\ 0 & 0 & 0 \\ 0 & 0 & -K \end{bmatrix},$$

$$\boldsymbol{\psi}(\boldsymbol{x}(t), \boldsymbol{x}(t-\tau)) = \begin{bmatrix} 0 \\ -x(t)z(t) \\ x(t-\tau)y(t) \end{bmatrix}, \quad K = 3.8,\ \tau_1 = 0.3,\ \tau_2 = 0.01.$$

Give the impulse control matrix $\boldsymbol{C} = diag(-0.2, -1.8, -1.8)$. The parameters l_1 and l_2 are selected as 4. The impulse interval is selected as $\varepsilon = 0.006$, so that the conditions of Theorem 2.2 can be satisfied. The initial states

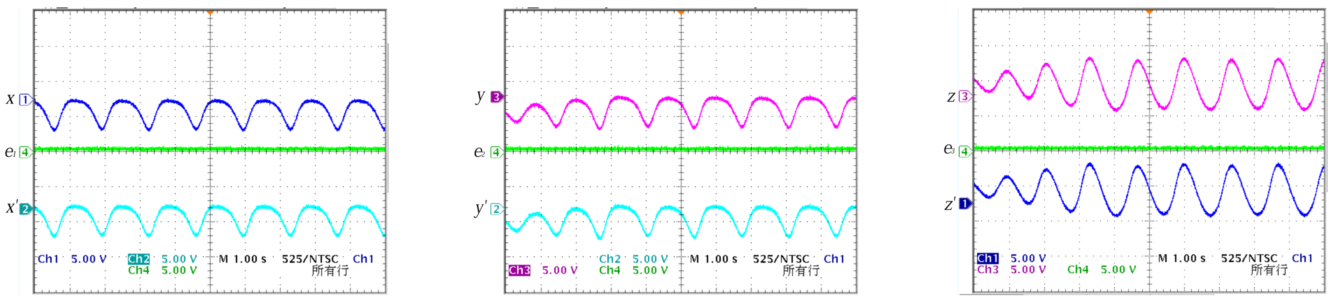

(a) The state of drive system x, response system x' and the error e_1 of the two systems after the controller is put into effect.

(b) The state of drive system y, response system y' and the error e_2 of the two systems after the controller is put into effect.

(c) The state of drive system z, response system z' and the error e_3 of the two systems after the controller is put into effect.

FIGURE 6. The experimental waveforms.

TABLE 2. Circuit component values.

Component	Value
R1, R4, R5, R6, R7, R9, R12, R13, R14, R15, R17, R20, R21, R22, R23	$1k\Omega$
R2	$1.2k\Omega$
R3, R11, R19	$12k\Omega$
R8, R16, R24	100Ω
R10, R18	$1.8k\Omega$

are $(\boldsymbol{x}(0), \boldsymbol{x}'(0)) = ((-0.1, -5, -0.1), (0.1, 1, 0.1))$. The simulation results are shown in Fig. 3, the impulse control starts from $t = 30s$. The subplot (a), (b)and (c) give the state errors e_1, e_2 and e_3, respectively. From Fig. 3, we know that the synchronization of the chaos systems with nonlinear time delays is achieved with the impulse controller.

C. CIRCUIT EXPERIMENTAL RESULTS

For the circuit schematic diagram of impulse synchronization, we use multipath selectors (CD4066) and operation amplifiers (LF347N) as shown in Fig. 4.

In Fig. 4, signal x, y and z are the state variables of the drive system, and x', y' and z' are the state variables of the response system. Let $\boldsymbol{e} = (e_1, e_2, e_3)^T$ be the synchronization error. The impulse control outputs are u_1, u_2 and u_3. The circuit parameters are summerized in Table 2. The 555 timer provides impulse signal with 10% duty ratio and 0.005s impulse interval. The block (a) in Fig. 4 is regard to the impulse gain $\boldsymbol{C}$ in Eq. (17), and the block (b) in Fig. 4 is used for signal power amplification. The switches in the Fig. 4 are employed as the multipath selector, on the moment that the switches are on-stated by a high level of 555 timer.

The circuit simulation results (using PSIM software) of the synchronization between the drive system and the response system are given in Fig. 5. The upper, middle and bottom subplot in Fig. 5 are the corresponding synchronization error curves e_1, e_2, e_3, respectively. Here, the impulse control is activated after $t = 80$ second. We can see, from Fig. 5, that the synchronization errors tend to zero after the controller is activated.

In the following, the circuit experiment is built to observe the synchronization between the two hyperchaotic systems. The experimental results are shown in Fig. 6.

The experiment results are presented as shown in Fig. 6. Fig. 6 (a), (b) and (c) illustrate the states of the two systems and the corresponding synchronization errors after the controller is put into effect. From Fig 6, we learn that the synchronization is verified by the experiment.

IV. CONCLUSION

To conclusion, based on Lyapunov stability theory, we proposed two theorems for impulse synchronization of the hyperchaotic systems with linear and nonlinear time delays, respectively. The proposed method has been applied to the Chen system with time delay to show its correctness and effectiveness of the theory from both the simulation and experiment results. The proposed theorems could be extended to paradigmatic systems with linear and nonlinear time delays. This method gives bright prospects to explore some realistic applications.

REFERENCES

[1] L. M. Pecora and T. L. Carroll, "Synchronization in chaotic systems," *Phys. Rev. Lett.*, vol. 64, no. 8, pp. 821–824, Feb. 1990.

[2] M. Lakshmanan and K. Murali, *Chaos in Nonlinear Oscillators: Controlling and Synchronization*. Singapore: World Scientific, 1996.

[3] Y.-C. Lai and C. Grebogi, "Synchronization of chaotic trajectories using control," *Phys. Rev. E, Stat. Phys. Plasmas Fluids Relat. Interdiscip. Top.*, vol. 47, no. 4, pp. 2357–2360, Apr. 1993.

[4] C. Huang and J. Cao, "Active control strategy for synchronization and anti-synchronization of a fractional chaotic financial system," *Phys. A, Stat. Mech. Appl.*, vol. 473, pp. 262–275, May 2017.

[5] M. T. Yassen, "Chaos synchronization between two different chaotic systems using active control," *Chaos, Solitons Fractals*, vol. 23, no. 1, pp. 131–140, Jan. 2005.

[6] X. Sun, H. Yu, J. Yu, and X. Liu, "Design and implementation of a novel adaptive backstepping control scheme for a PMSM with unknown load torque," *IET Electr. Power Appl.*, vol. 13, no. 4, pp. 445–455, Apr. 2019.

[7] D. Pucci, T. Hamel, P. Morin, and C. Samson, "Nonlinear feedback control of axisymmetric aerial vehicles," *Automatica*, vol. 53, pp. 72–78, Mar. 2015.

[8] S. Hao, P. H. Ju, Z. G. Wu, and Z. Q. Zhang, "Finite-time H_∞ synchronization for complex networks with semi-Markov jump topology," *Commun. Nonlinear Sci. Numer. Simul.*, vol. 24, pp. 40–51, Jul. 2015.
[9] Q. Ye, Z. Jiang, and T. Chen, "Adaptive feedback control for synchronization of chaotic neural systems with parameter mismatches," *Complexity*, vol. 2018, pp. 1–8, Sep. 2018.
[10] J. Ma, W. T. Su, and J. Z. Gao, "Optimization of self-adaptive synchronization and parameters estimation in chaotic Hindmarsh-Rose neuron model," (in Chinese), *Acta Phys. Sinica*, vol. 59, pp. 1554–1561, Mar. 2010.
[11] L. Fang, T. Li, Z. Li, and R. Li, "Adaptive terminal sliding mode control for anti-synchronization of uncertain chaotic systems," *Nonlinear Dyn.*, vol. 74, no. 4, pp. 991–1002, Dec. 2013.
[12] T. Yang, "Impulsive control," *IEEE Trans. Autom. Control*, vol. 44, no. 5, pp. 1081–1083, May 1999.
[13] D. Cafagna and G. Grassi, "Fractional-order systems without equilibria: The first example of hyperchaos and its application to synchronization," *Chin. Phys. B*, vol. 24, no. 8, Aug. 2015, Art. no. 080502.
[14] T. A. Ahmad, S. Vaidyanathan, and A. Ouannas, *Fractional Order Control and Synchronization of Chaotic Systems*. Cham, Switzerland: Springer, 2017.
[15] M.-F. Danca and N. Kuznetsov, "Parameter switching synchronization," *Appl. Math. Comput.*, vol. 313, pp. 94–102, Nov. 2017.
[16] M. S. Santos, J. D. Szezech, F. S. Borges, K. C. Iarosz, I. L. Caldas, A. M. Batista, R. L. Viana, and J. Kurths, "Chimera-like states in a neuronal network model of the cat brain," *Chaos, Solitons Fractals*, vol. 101, pp. 86–91, Aug. 2017.
[17] H.-P. Ren and C. Bai, "Secure communication based on spatiotemporal chaos," *Chin. Phys. B*, vol. 24, no. 8, Aug. 2015, Art. no. 080503.
[18] B. Wang, S. M. Zhong, and X. C. Dong, "On the novel chaotic secure communication scheme design," *Commun. Nonlinear Sci. Numer. Simul.*, vol. 39, pp. 108–117, Oct. 2016.
[19] H. P. Ren, "A method of realizing single direction chaotic rotation speed of permanent magnet synchronous motor is provided powered by a threephase full-bridge inverter," Amer. Patent Appl. PCT/CN 073 418, Mar. 19, 2019.
[20] J. Hu, H. Zhang, X. Yu, H. Liu, and D. Chen, "Design of sliding-mode-based control for nonlinear systems with mixed-delays and packet losses under uncertain missing probability," *IEEE Trans. Syst., Man, Cybern. Syst.*, early access, Jun. 13, 2019, doi: 10.1109/TSMC.2019.2919513.
[21] H. R. Karimi and H. J. Gao, "New delay-dependent exponential H_∞ synchronization for uncertain neural networks with mixed time delays," *IEEE Trans. Syst., Man, Cybern. B, Cybern.*, vol. 40, no. 1, pp. 173–185, Feb. 2010.
[22] H.-P. Ren, C. Bai, K. Tian, and C. Grebogi, "Dynamics of delay induced composite multi-scroll attractor and its application in encryption," *Int. J. Non-Linear Mech.*, vol. 94, pp. 334–342, Sep. 2017.
[23] S. Banerjee and R. R. Sarkar, "Delay-induced model for tumor–immune interaction and control of malignant tumor growth," *Biosystems*, vol. 91, no. 1, pp. 268–288, Jan. 2008.
[24] H. P. Ren, D. Liu, and C. Z. Han, "Anticontrol of chaos via direct time delay feedback," *Acta Phys. Sinica*, (in Chinese), vol. 55, pp. 2694–2701, Jun. 2006.
[25] K. Tian, H.-P. Ren, and C. Grebogi, "Existence of chaos in the Chen system with linear time-delay feedback," *Int. J. Bifurcation Chaos*, vol. 29, no. 9, Aug. 2019, Art. no. 1950114.
[26] H.-P. Ren, K. Tian, and C. Grebogi, "Topological horseshoe in a single-scroll Chen system with time delay," *Chaos, Solitons Fractals*, vol. 132, Mar. 2020, Art. no. 109593.
[27] H. P. Ren and W. C. Li, "Heteroclinic orbits in chen circuit with time delay," *Commun. Nonlinear Sci. Numer. Simul.*, vol. 15, no. 10, pp. 3058–3066, Oct. 2010.
[28] T. Yang and L. O. Chua, "Impulsive stabilization for control and synchronization of chaotic systems: Theory and application to secure communication," *IEEE Trans. Circuits Syst. I, Fundam. Theory Appl.*, vol. 44, no. 10, pp. 976–988, Nov. 1997.
[29] W. He, X. Gao, W. Zhong, and F. Qian, "Secure impulsive synchronization control of multi-agent systems under deception attacks," *Inf. Sci.*, vol. 459, pp. 354–368, Aug. 2018.
[30] W. He, F. Qian, and J. Cao, "Pinning-controlled synchronization of delayed neural networks with distributed-delay coupling via impulsive control," *Neural Netw.*, vol. 85, pp. 1–9, Jan. 2017.
[31] X. Z. Liu and G. Ballinger, "Uniform asymptotic stability of impulsive delay differential equation," *Comput. Math. Appl.*, vol. 41, pp. 903–915, Apr. 2001.
[32] C. Li, X. Liao, and R. Zhang, "A unified approach for impulsive lag synchronization of chaotic systems with time delay," *Chaos, Solitons Fractals*, vol. 23, no. 4, pp. 1177–1184, Feb. 2005.
[33] Z. Wu, D. Liu, and Q. Ye, "Pinning impulsive synchronization of complex-variable dynamical network," *Commun. Nonlinear Sci. Numer. Simul.*, vol. 20, no. 1, pp. 273–280, Jan. 2015.
[34] X. Li, J. Cao, and D. W. C. Ho, "Impulsive control of nonlinear systems with time-varying delay and applications," *IEEE Trans. Cybern.*, early access, Feb. 13, 2019, doi: 10.1109/TCYB.2019.2896340.

KUN TIAN was born in Hebei, China, in 1989. She received the master's degree in control science and engineering from the Xi'an University of Technology, in 2016, where she is currently pursuing the Ph.D. degree. She has published four journal articles.

HAI-PENG REN (Member, IEEE) was born in Heilongjiang, China, in March 1975. He received the Ph.D. degree from the Xi'an University of Technology, in 2003.

He worked with Kyushu University, Japan, Xi'an Jiaotong University, and the University of Aberdeen, U.K. He has been a Professor with the Xi'an University of Technology, since November 2008. He has published more than 150 journal articles and conference papers. His research interests include nonlinear system control, complex networks, communication with nonlinear dynamics, and system biology.

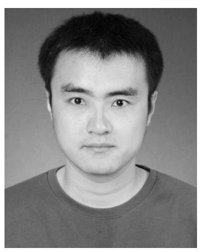

CHAO BAI was born in Xi'an, China, in 1988. He received the B.S. degree in automation from Xi'an Polytechnic University, in 2010, and the M.S. and Ph.D. degrees in control science and engineering from the Xi'an University of Technology. His current research interests include chaotic communication and complex networks.